International Conferences on Recent Advances in Geotechnical Earthquake Engineering and Soil Dynamics

1995 - Third International Conference on Recent Advances in Geotechnical Earthquake Engineering & Soil Dynamics

06 Apr 1995, 10:30 am - 12:30 pm

Area of Compaction to Prevent Uplift by Liquefaction

Yukihisa Tanaka
Central Research Institute of Electric Power Industry, Japan

Hideo Komine
Central Research Institute of Electric Power Industry, Japan

Jun-ichi Tohma
Central Research Institute of Electric Power Industry, Japan

Keizo Ohtomo
Central Research Institute of Electric Power Industry, Japan

Hitoshi Tochigi
Central Research Institute of Electric Power Industry, Japan

See next page for additional authors

Recommended Citation

Author

Yukihisa Tanaka, Hideo Komine, Jun-ichi Tohma, Keizo Ohtomo, Hitoshi Tochigi, Hidenori Abo, and Satoyuki Fukuda

Area of Compaction to Prevent Uplift by Liquefaction

Paper No. 3.34

Yukihisa Tanaka, Hideo Komine, Jun-ichi Tohma, Keizo Ohtomo, and Hitoshi Tochigi
Central Research Institute of Electric Power Industry

Hidenori Abo and Satoyuki Fukuda
Tokyo Electric Power Company

SYNOPSIS   In this study, shaking table tests, upper seepage flow tests and numerical analyses were conducted to determine the condition of improvement by the compaction method, including the extent of area and the density, to prevent uplift of underground pipes by liquefaction. Based on the results of these investigations, a procedure to determine the improvement conditions was proposed.

INTRODUCTION

In Japan, since underground pipes are often laid in liquefiable sand deposits, remedial treatment of the surrounding ground is necessary and the compaction method is usually used. For this, it is important to determine the extent as well as the target density of the improved area because of restrictions on the area and cost of earth work. In this study, upper seepage flow tests, shaking table tests and numerical analyses were conducted to determine the conditions of improvement.

EXPERIMENT

Upward Seepage Flow Test

Upward seepage flow tests were conducted using a one-tenth model to investigate the effect of hydraulic gradient and density of the model ground on uplift behavior of the underground pipe. Figure 1 shows the schematic view of the upward seepage flow test. For accurate measurement, pore pressure for evaluating the average pore water pressure ratio in the ground was measured using a pore pressure meter installed at the bottom of the sand layer. Sengenyama sand with a grain size distribution as shown in Fig. 2 and physical properties as shown in Table 1 was used in this series of tests. Table 2 lists the conditions of the experiments.

Figure 3 shows the relationship between the amount of uplifting and average pore pressure ratio of the ground obtained by the upward seepage flow test. The amount of uplift was measured after transient movement of the underground pipe, which was triggered by increasing the hydraulic gradient, ceased. Thus the relationship was thought to be obtained under drained condition. The amount of uplifting increases with increasing average pore pressure ratio in Fig. 3. - The threshold value of the average pore pressure ratio corresponding to uplift seems to be 0.7~0.8. If the average pore pressure ratio increases beyond the threshold values, the amount of uplift becomes unlimited until the underground pipe rises up to the ground surface. The solid symbols approximate the upper limit of the pore pressure ratio inside which the
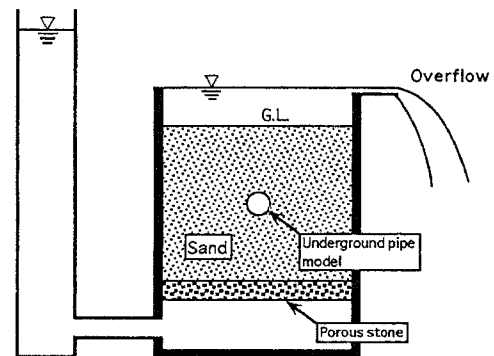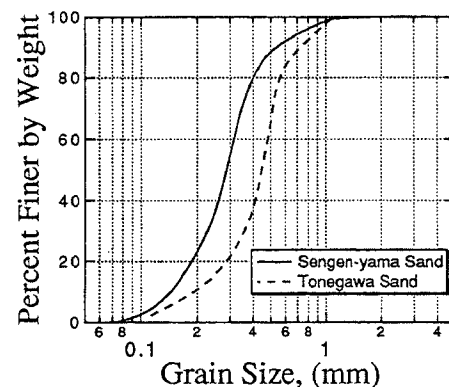

Fig.1. Schematic View of Upward Seepage Flow Test

Fig.2. Grain Size Distributions of Sands

amount of uplift doesn't become very large(Komine and Tanaka, 1991).

Shaking Table Test

Figure 4 shows a cross section of the model ground, using a one-fifth scale model. The model underground pipes of 12cm diameter are buried in the compacted area near the center of the model container at a depth of 30cm.

Table 1. Physical Properties of Sands

Physical Properties	Sengen-yama Sand	Tonegawa Sand
Maximum Grain Size D_{max} (mm)	2.00	2.00
Average Grain Size D_{50} (mm)	0.285	0.32
Uniformity Coefficient, U_c	2.116	2.500
Specific Gravity, G_s	2.703	2.718
Maximum Dry Density ρ_{dmax} (g/cm³)	1.702	1.652
Minimum Dry Density ρ_{dmin} (g/cm³)	1.395	1.329
Minimum Void Ratio, e_{min}	0.588	0.645
Maximum Dry Density, e_{max}	0.938	1.045

Table 2. Test Conditions

Upward Seepage Flow Test			Shaking Table Test	
Cases	Dry density ρd (g/cm²)	Relative density Dr (%)	Cases	Width of the Improved Part, B (cm)	Relative Density, Dr (%) of the Improved Part
A	1.483	33	1	0 (Un-improved ground)	30
B	1.533	50	2	60	69
C	1.591	68	3	90	87
			4	120	66

Table 2 lists the conditions of the experiments. In this series of tests, the effect of the extent of the improved area on the behavior of the underground pipe model was investigated. Tonegawa sand, with a grain size distribution as shown in Fig. 2, was used in this series of tests.

Figure 5 shows the relationship between the amount of uplifting of the buried pipes and pore pressure ratio, ru, acting on the bottom of the pipes immediately after seismic excitation. It should be noted that pore pressure at the bottom of the underground pipe was interpolated by the pore pressures measured in the surrounding ground because the pore pressure measured at the bottom of the underground pipe is affected by movement of the pipe and locality of the distribution of pore pressure around the pipe.

The amount of uplifting in Case-3 and Case-4 is very small, while that in Case-1 and Case-2 increases with increasing pore pressure ratio. The threshold value of the average pore pressure ratio corresponding to uplift seems to be 0.7～0.8, which is the same as the threshold value obtained in the upward seepage flow test described previously(Tochigi, et al. 1991).

PORE PRESSURE RATIO OF UPLIFT

Mechanism of Uplifting

To investigate the mechanism of uplift of the underground pipe, we assume that the slip surfaces due to uplift as shown in Fig.6, which are similar to the Japanese standard, "Design Manual for Common Utility Ducts" to investigate uplift of rectangular common utility ducts.

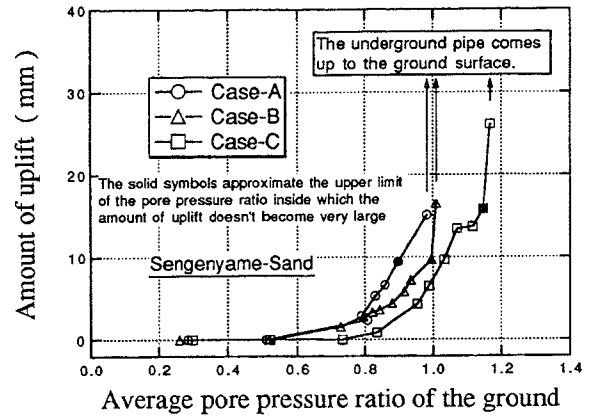Assuming that the pore water pressure ratio is

Fig.3. Uplift vs. Average Pore Pressure Ratio (Results of Upward Seepage Flow Test)

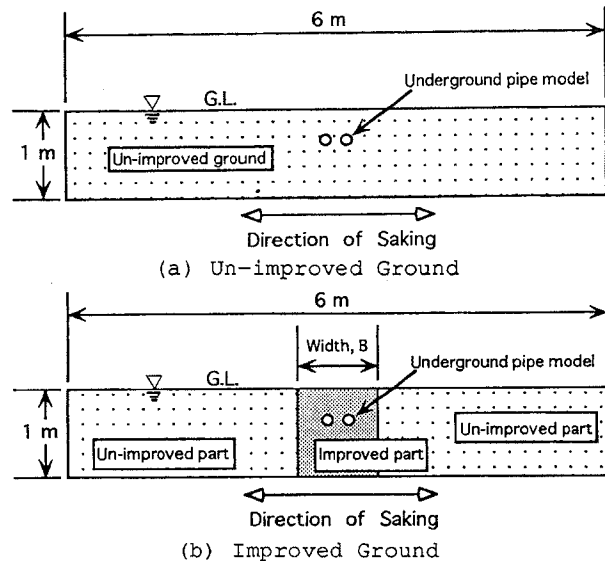

(a) Un-improved Ground

(b) Improved Ground
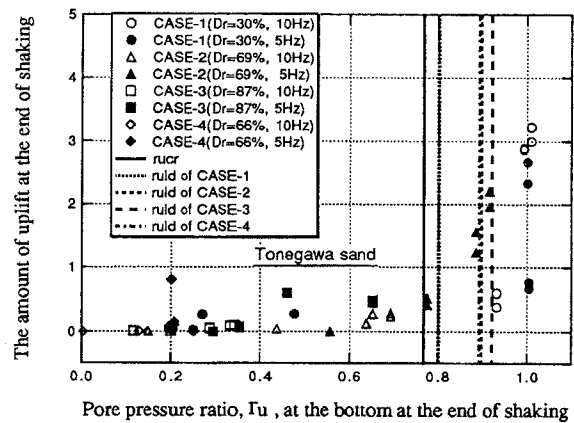Fig.4. Schematic View of Shaking Table Test

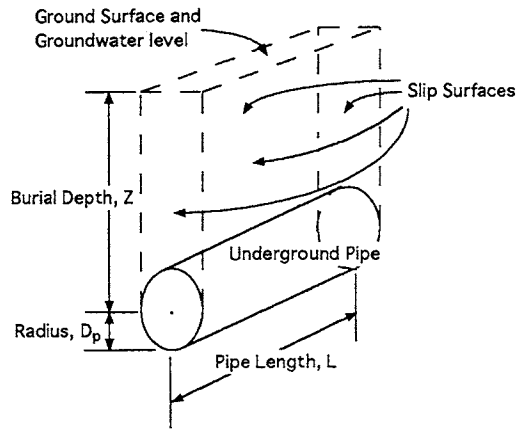Fig.5. Uplift vs. Pore Pressure Ratio (Results of Shaking Table Test)

Fig.6. Assumed Slip Surfaces due to Uplift

constant throughout the ground, the uplift force due to pore water pressure acting on the bottom of the buried pipes is given by:

$$U = L \cdot \int_0^{\pi} (Z + \frac{Dp}{2} \sin \theta) \cdot (\gamma_w + r_u \gamma') \cdot \frac{Dp}{2} \sin \theta \cdot d\theta$$

$$= n \frac{D_P^2}{2} \cdot (\gamma_w + r_u \gamma') \cdot (2Z + \frac{\pi}{4} Dp)$$

(1)

Where,
γ_w: Unit weight of water
γ': Submerged unit weight of surrounding sand
Dp: Diameter of the underground pipe
Z: Buried depth
n: L/Dp (L:Length of underground pipe)
ru:Excess pore water pressure ratio in the ground

The self-weight of the underground pipe, W1, is given by:

$$W_1 = n \frac{\pi}{4} D_P^3 Gp \gamma_w$$

(2)

Where,
Gp: Apparent specific gravity of underground pipe, which is unity in this series of tests.

$$Gp = 1$$

(3)

Assuming that the failure surfaces by uplifting is as shown in Fig. 6, the self-weight of the soil surrounded by four failure planes , W2, is given by:

$$W_2 = nDp(ZDp - \frac{\pi}{8} D_P^2) \cdot (\gamma' + \gamma_w)$$

(4)

The shear resistance force along the vertical failure planes and both sides of the underground pipe model, T, is given by:

$$T = (1+n)DpZ^2 \gamma K(1-r_u) \tan \phi'$$

(5)

Where,

K: Coefficient of earth pressure (= σ_h'/σ_v', σ_h': Horizontal earth pressure, σ_v': Vertical earth pressure)

For equilibrium of the forces acting on the underground pipes then:

$$U = W_1 + W_2 + T$$

(6)

Substituting Eqs.(1),(2),(4) and (5) into Eq.(6), we get the following equation:

$$r_{uld} = \frac{n \frac{\pi}{4}(Gp-1)\frac{\gamma_w}{\gamma'} + n(t - \frac{\pi}{8}) + (1+n)t^2 K \tan \phi'}{n(t + \frac{\pi}{8}) + (1+n)t^2 K \tan \phi'}$$

(7)

ruld in Eq.(7) corresponds to the pore pressure ratio causing large amount of uplift because shear resistance of the ground was taken into account in Eq.(7). In the early stage of uplift, since the shear resistance acting on the vertical slip planes is not mobilized, Eq.(7) is rewritten as follows:

$$r_{ucr} = \frac{\frac{\pi}{4}(Gp-1)\frac{\gamma_w}{\gamma'} + (t - \frac{\pi}{8})}{t + \frac{\pi}{8}}$$

(8)

The relationship between internal friction angle, ϕ', and relative density, Dr, is assumed to be given by(Shimobe and Miyamori, 1991):

$$\phi' = 33.5 + (0.041Dr^2 + 6.13Dr) \times 10^{-2}$$

(9)

where,
ϕ': internal friction angle (deg)
Dr: relative density (%)

In Fig. 7, the results of calculation by Eq.(7) with Gp=1, n=3.58, t=3.33 and K=0.5, is shown by the dotted line. The observed ruld values, which correspond to solid symbols in Fig.3, increases sharply with increasing relative density, Dr, whereas the calculated value increases slightly. This difference may be attributed to localization of shear failure in loose sand deposit.

The observed value of ruld becomes unity or more if the relative density exceeds 50%. This is due to the heterogeneous distribution of excess pore water pressure in the model ground. The presence of the underground pipe reduces the excess pore water pressure above the underground pipe than that at the same depth.

To model the heterogeneous distribution of excess pore water pressure and locality of failure, parameters α and β are introduced. The average pore pressure ratio above the underground pipe is assumed to be α times the average pore pressure ratio in the ground. The failure planes are assumed to occur from depth Z, while the vertical length of the failure plane is expressed as βZ, where the value of β is assumed to be a function of the relative density. Using α and β, Eq.(7) is rewritten as follows:
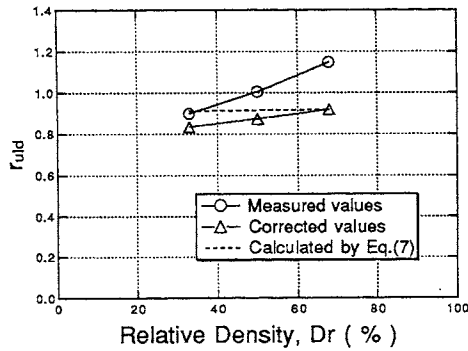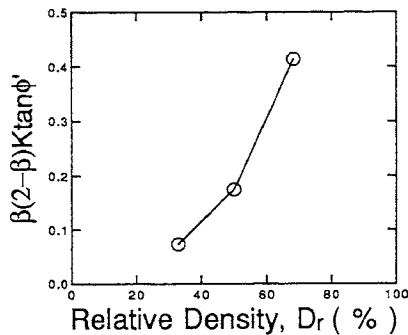
Fig.7. r_{uld} vs. Dr

Fig.8. $\beta(2-\beta)K\tan\phi'$ vs. Dr

$$r_{uld}=\frac{n\frac{\pi}{4}(Gp-1)\frac{\gamma w}{\gamma}+n(t-\frac{\pi}{8})+\beta(2-\beta)(1+n)t^2K\tan\phi'}{n(t+\frac{\pi}{8})+\alpha\beta(2-\beta)(1+n)t^2K\tan\phi'}$$

(10)

Substituting $\beta=1$ and the observed r_{uld} value of Case-C which corresponds to a solid square in Fig.3 into Eq.(10), $\alpha=0.67$ was obtained. Since the value of α seems independent of the relative density of the ground, $\alpha=0.67$ can be used to calculate the values of β of Cases A and B.

According to the result of seepage flow analysis which was conducted to know the pore pressure distribution in the improved part when the the un-improved part completely liquefied, pore pressure ratio along the axis of symmetry in Fig.9 does not change so much if z/H is less than 0.6(Komine and Tanaka, 1991). Thus it is reasonable to assume $\alpha=1.0$ in the region of z/H< 0.6. Substituting $\alpha=1.0$ and the values of β calculated above into Eq.(10) with Gp=1, the corrected values of r_{uld} of Cases A, B and C were calculated. These results are plotted in Fig. 7 as open triangles.

Since the parameters, β and ϕ' are functions of Dr, $\beta(2-\beta)\tan\phi'$ in Eq.(10) is a function of Dr. Figure 8 shows the relationship between $\beta(2-\beta)K\tan\phi'$ with K=0.5 and the relative density of the ground, Dr.

Appropriateness of r_{ucr} and r_{uld} for Uplift during Shaking

The calculated r_{uld} and r_{ucr} values using Eqs.(7) and (8) with Gp=1 and Fig.8 are plotted as vertical lines in Fig. 5. Although in the shaking table tests the uplift occurred only
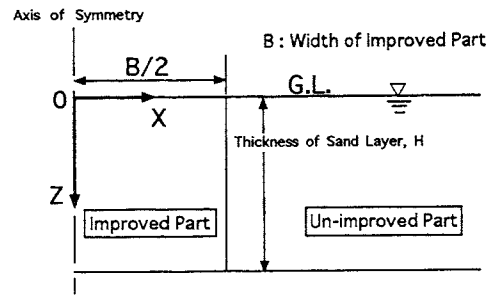

Fig.9. Schematic View of Improved Ground

during shaking, the r_{uld} and r_{ucr} values seem to correspond to the threshold uplift and large amount of uplift, respectively.

NUMERICAL ANALYSIS

The generation and dissipation of pore water pressure was analyzed using a computer program modified from GADFLEA(Booker, et al. 1976), the basic equation of which is a consolidation equation similar to the equation of heat conduction.

Figure 9 shows a cross section of the ground used for the numerical analysis. As shown in Fig. 9 , the presence of underground pipes were not considered for the numerical analysis in order to enhance the generality of the calculated results. For simplicity, the permeability and the volumetric compressibility of the improved part and the un-improved part are assumed to be constant in each part.

Simplification of the Problem

The basic equations of the analysis are as follows:

$$C_{VDX}\frac{\partial^2 u_D}{\partial x^2}+C_{VDZ}\frac{\partial^2 u_D}{\partial z^2}=\frac{\partial u_D}{\partial t}-\frac{\partial u_{gD}}{\partial t}$$

$$C_{VLX}\frac{\partial^2 u_L}{\partial x^2}+C_{VLZ}\frac{\partial^2 u_L}{\partial z^2}=\frac{\partial u_L}{\partial t}-\frac{\partial u_{gL}}{\partial t}$$

(11a), (11b)

Where,

C_{VDX}, C_{VLX}: Coefficient of consolidation in the X direction of the improved part and the un-improved part, respectively.

C_{VDZ}, C_{VLZ}: Coefficient of consolidation in the Z direction of the improved part and the un-improved part, respectively.

u_D, u_L: Excess pore water pressure in the improved part and the un-improved part, respectively.

u_{gD}, u_{gL}: Excess pore water pressure generated by cyclic shear in the improved part and the un-improved part, respectively.

The boundary conditions are as follows:

$\partial u_D/\partial x=0$	at x=0	(12a)
$\partial u_L/\partial x=0$	at x=∞	(12b)
$\partial u_D/\partial z=\partial u_L/\partial z=0$	at z=H	(12c)
$u_D=u_L=0$	at z=0	(12d)
$u_D=u_L$	at x=B/2	(12e)

The initial conditions are as follows:

$u_D=u_L=0$	at t=0	(13)

The problem defined by Eqs.(11),(12) and (13) can be divided into the following two problems.

I. Excess pore pressure by cyclic shear is generated only in the un-improved part.
II. Excess pore pressure by cyclic shear is generated only in the improved part.

The basic equations governing problem-I above are as follows:

$$C_{VDX}\frac{\partial^2 u_{D1}}{\partial x^2} + C_{VDZ}\frac{\partial^2 u_{D1}}{\partial z^2} = \frac{\partial u_{D1}}{\partial t}$$

$$C_{VLX}\frac{\partial^2 u_{L1}}{\partial x^2} + C_{VLZ}\frac{\partial^2 u_{L1}}{\partial z^2} = \frac{\partial u_{L1}}{\partial t} - \frac{\partial u_{gL1}}{\partial t}$$

$$(14a), (14b)$$

The boundary conditions are as follows:

$\partial u_{D1}/\partial x=0$	at x=0	(15a)
$\partial u_{L1}/\partial x=0$	at x=∞	(15b)
$\partial u_{D1}/\partial z=\partial u_{L1}/\partial z=0$	at z=H	(15c)
$u_{D1}=u_{L1}=0$	at z=0	(15d)
$u_{D1}=u_{L1}$	at x=B/2	(15e)

The initial value as follows:

$$u_{D1}=u_{L1}=0 \qquad \text{at } t=0 \qquad (16)$$

On the other hand, the basic equations governing problem-II above are as follows:

$$C_{VDX}\frac{\partial^2 u_{D2}}{\partial x^2} + C_{VDZ}\frac{\partial^2 u_{D2}}{\partial x^2} = \frac{\partial u_{D2}}{\partial t} - \frac{\partial u_{gD2}}{\partial t}$$

$$C_{VLX}\frac{\partial^2 u_{L2}}{\partial x^2} + C_{VLZ}\frac{\partial^2 u_{L2}}{\partial z^2} = \frac{\partial u_{L2}}{\partial t}$$

$$(17a), (17b)$$

The boundary conditions are as follows:

$\partial u_{D2}/\partial x=0$	at x=0	(18a)
$\partial u_{L2}/\partial x=0$	at x=∞	(18b)
$\partial u_{D2}/\partial z=\partial u_{L2}/\partial z=0$	at z=H	(18c)
$u_{D2}=u_{L2}=0$	at z=0	(18d)
$u_{D2}=u_{L2}$	at x=B/2	(18e)

The initial conditions are as follows:

$$u_{D2}=u_{L2}=0 \qquad \text{at } t=0 \qquad (19)$$

Adding Eq.(14) to Eq.(17), we obtain the following equations.

$$C_{VDX}\frac{\partial^2 (u_{D1}+u_{D2})}{\partial x^2} + C_{VDZ}\frac{\partial^2 (u_{D1}+u_{D2})}{\partial x^2} = \frac{\partial (u_{D1}+u_{D2})}{\partial t} - \frac{\partial u_{gD2}}{\partial t}$$

$$C_{VLX}\frac{\partial^2 (u_{L1}+u_{L2})}{\partial x^2} + C_{VLZ}\frac{\partial^2 (u_{L1}+u_{L2})}{\partial z^2} = \frac{\partial (u_{L1}+u_{L2})}{\partial t} - \frac{\partial u_{gL1}}{\partial t}$$

$$(20a), (20b)$$

For the boundary conditions, we obtain the following equations by adding Eqs.(15) to Eqs.(18).

$\partial (u_{D1}+u_{D2})/\partial x=0$	at x=0	(21a)
$\partial (u_{L1}+u_{L2})/\partial x=0$	at x=∞	(21b)
$\partial (u_{D1}+u_{D2})/\partial z=\partial (u_{L1}+u_{L2})/\partial z=0$	at z=H	(21c)
$u_{D1}+u_{D2}=u_{L1}+u_{L2}=0$	at z=0	(21d)
$u_{D1}+u_{D2}=u_{L1}+u_{L2}$	at x=B/2	(21e)

The following equation can also be obtained as an initial condition by adding Eqs.(16) to Eqs.(19).

$$u_{D1}+u_{D2}=u_{L1}+u_{L2}=0 \qquad \text{at } t=0 \qquad (22)$$

By comparing Eqs.(11),(12) and (13) to Eqs.(20),(21) and (22), replacing $u_{D1}+u_{D2}$ for u_D and $u_{L1}+u_{L2}$ for u_L, these equations appear to be the same. However, one should note that the terms of pore pressure generation are generally different as shown below because the pore pressure generated per unit time is assumed to be affected by the total pore pressure ratio in GADFLEA(Booker, et al. 1976).

$$\partial u_{gD}/\partial t \neq \partial u_{gD2}/\partial t \qquad (23a)$$
$$\partial u_{gL}/\partial t \neq \partial u_{gL1}/\partial t \qquad (23b)$$

However, we can make Eqs.(20a) and (20b) exactly the same as Eqs.(11a) and (11b) by assuming that the pore pressure generated per unit time is independent of the total pore pressure ratio, as shown below:

$$\partial u_g/\partial t = Nc/N\ell \qquad (24)$$

Where,
Nc: Number of cycles
$N\ell$: Number of cycles required to reach liquefaction

The solution of the problem expressed by Eqs.(11), (12), (13) can thus be approximately obtained as the sum of the solutions of problem-I and problem-II(Komine and Tanaka, 1991; Tanaka, et al. 1991).

Maximum Pore Pressure in Improved Part after Termination of Seismic Motion

According to the results of the shaking table tests conducted in this study, the underground pipe is uplifted only during shaking because in the scale model test the distance between the underground pipe and the liquefied part is rather small. However, in actual ground, liquefaction is thought to occur under almost undrained conditions and dissipation to occur only after termination of seismic motion. Therefore it is very important to consider uplift of the underground pipe after earthquake motion.

To investigate the effect of seepage flow from the liquefied un-improved part into the non-liquefied improved part, numerical analysis using the computer program GADFLEA was conducted. The initial conditions of the analysis are as follows:

ru=0 for the improved part at t=0
ru=1 for the un-improved part at t=0

In reality, even in the improved part of the ground, pore pressure generation occurs to some degree by cyclic shear during earthquake motion and by increase in horizontal earth pressure due to liquefaction of the un-improved ground. However, it dissipates more quickly than that generated in the un-improved part of the ground because the coefficient of volumetric compressibility and the drainage length of the improved part are much smaller than those of the un-improved part.

Analysis Results

Figure 10 shows the effect of k_{DZ}/k_{LZ} and m_{VD}/m_{VL} on the maximum pore pressure ratio at X=0, z=0.4H. The pore pressure ratio increases as the
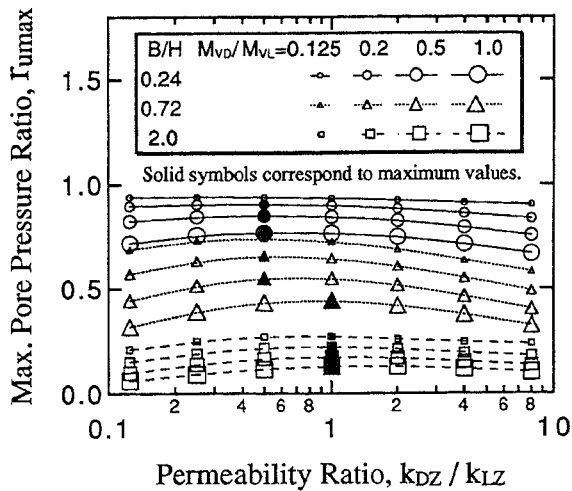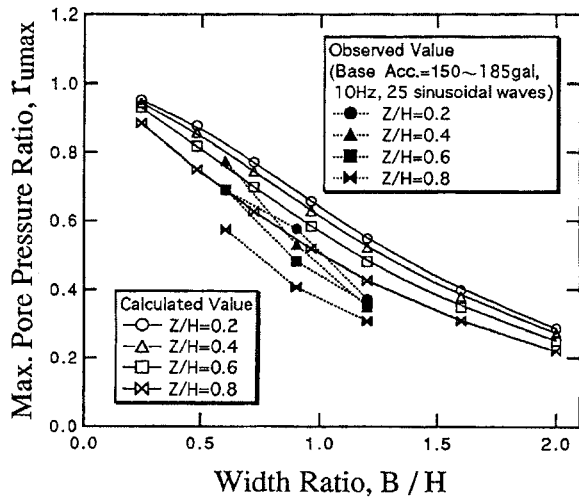
273

Fig.10. rumax vs. kDZ/kLZ

Fig.11. rumax of $m_{VD}/m_{VL}=0.125$ vs.B/H

REFERENCES

Booker, J.R., Rahman, M.S. and Seed, H.B. (1976), "GADFLEA—A Computer Program for the Analysis of Pore Pressure Generation and Dissipation during Cyclic or Earthquake Loading", EERC 76-24.

Japan Road Association (1986), Design Manual for Common utility Ducts.(in Japanese)

Komine, H. and Tanaka, Y.(1991), "Investigation on Countermeasure against Liquefaction for Underground Pipe(Part2), —Design Method of Effective Ground Compaction Width—", Report No.U91045, Central Research Institute of Electric Power Industry(in Japanese).

Simobe, S. and Miyamori, T. (1991), "The Relationships of Internal Friction Angles Obtained by Triaxial Test, Plane Strain Test and Direct Shear Test", Proc. of the Symposium on Procedure of Triaxial Test, JSSMFE, pp.209-216(in Japanese).

Tanaka, Y., Komine, H., Tochigi, H., Tohma, J., Ohtomo, K., Fukuda, S. and Abo, H. (1991), "A Study on Ground Compaction for Buried Pipes as Remedial measures against Liquefaction(Part 3), —Numerical Analysis—", 21th Earthquake Engineering Research Conference, JSCE, pp.257 - 260(in Japanese).

Tochigi, H., Tohma, J. and Ohtomo, K.(1991), "Investigation on Countermeasure against Liquefaction for Underground Pipe(Part1),— Confirmation of Effectiveness of the Countermeasure by Shaking Table Tests—", Report No.U91501, Central Research Institute of Electric Power Industry(in Japanese).

ratio m_{VD}/m_{VL} decreases, whereas the pore pressure ratio has a maximum when the ratio k_{DZ}/k_{LZ} varies from 0.125 to 8. These values are almost the minimum and maximum values of m_{VD}/m_{VL}, respectively(komine and Tanaka, 1991). Figure 11 shows the maximum pore pressure at X=0 when $m_{VD}/m_{VL}=0.125$ plotted against B/H. In laboratory cyclic shear tests, 0.125 seems to be almost the smallest value of m_{VD}/m_{VL}. Thus the maximum pore pressure in Fig. 11 seems to be the maximum value of each B/H. In Fig.11, observed values from the shaking table tests are also plotted as solid symbols. Though the un-improved part liquefied completely in the shaking table tests, all the observed pore pressure ratios are smaller than the calculated values. Thus the calculated values in Fig. 11 can be used for safer design.

PROCEDURE TO DETERMINE B/H VALUE

We can determine the area of compaction to prevent uplift of underground pipes due to liquefaction using Eqs.(8) and (10) with $\alpha=1$ and Figs.8 and 11 when the values of G_P, n, t, Dr are given as design conditions.